Nuclear Physics B122 (1977) 464–484

THE ROLE OF A_1 EXCHANGE IN THE REACTION $\pi^- p \to (\pi^+\pi^-)n$ *

J.D. KIMEL and J.F. OWENS
Department of Physics, Florida State University, Tallahassee, Florida 32306

Received 25 October 1976
(Revised 15 February 1977)

Data have recently become available, at 17.2 GeV/c, which show strong target polarization effects for the reaction $\pi^- p \to (\pi^+\pi^-)n$. These data require the presence of an exchange with the quantum numbers of the A_1. A simple model based on π, A_2, and A_1 Regge pole exchange together with parametrized $n = 0$ cuts is found to provide an excellent description of both the polarized and unpolarized data. The resulting structure of the A_1 dominated amplitudes is discussed and the results are compared with earlier models which neglected A_1 exchange effects.

1. Introduction

The reaction

$$\pi^- p \to (\pi^+\pi^-)n \tag{1}$$

has long been an important source of information concerning the dynamics of strong interaction processes. Much of our knowledge of $\pi\pi$ phase shifts has been obtained by studying reaction (1) and other related reactions [1]. In addition, the spin information obtained from the various density matrix elements has enabled this reaction to play a crucial role in testing models of quasi-two-body interactions [2]. In the past several years high statistics data for reaction (1) at 17.2 GeV/c [3] have been used both for $\pi\pi$ phase shift analyses [4] and for studying the dynamics of resonance production [5]. A feature common to all of these analyses has been the assumption that the A_1 exchange contribution was negligible. This assumption reduces the number of independent helicity amplitudes, thereby allowing model dependent amplitude analyses to be performed.

Preliminary data, obtained with a polarized target, have recently been presented for reaction (1) at 17.2 GeV/c [6]. The additional observables available as a result of the polarized target are sensitive to the presence of an exchange with the quantum numbers of the A_1. Unexpectedly large polarization effects are seen in the data, thereby calling for a reassessment of previous analyses which neglected A_1 exchange.

* Work supported in part by the US Energy Research and Development Administration.

In this paper we present results of an analysis using the data of refs. [4] and [6] at 17.2 GeV/c together with preliminary data at 6 GeV/c [7]. The model used is an extension of that presented in ref. [5]. Reggeized π, A_2, and A_1 exchanges are included as well as Regge cuts in amplitudes with zero net helicity flip in the s channel. The addition of A_1 exchange results in a good description of the new polarization data. Furthermore, the A_1 exchange terms improve the description of the unpolarized data, particularly in the large t region ($0.5 \lesssim -t \lesssim 1$ (GeV/c)^2).

In sect. 2 a brief review of the formalism used to describe target polarization data is given. In sect. 3 the model is presented and the results of the fit are discussed in sect. 4. In sect. 5 various alternatives to A_1 exchange are discussed and our conclusions are presented in sect. 6. The relations between the observables used in this analysis and the moments of the $\pi\pi$ angular distribution are given in the appendix, along with the expressions for these observables in terms of definite naturality amplitudes.

2. Observables

In this section a short review of the formalism for analyzing polarized target observables is given. In the following, only s- and p-wave dipion systems will be considered, although the results are easily generalized to higher partial waves. The observables are expressed in terms of s-channel helicity amplitudes *, $f_{\mu\lambda',\lambda}$, where λ and λ' denote the initial and final nucleon helicities respectively. The helicity of the dipion system is designated by μ with μ = s denoting an s-wave system.

The s-channel c.m. coordinate system used to describe the target polarization vector is shown in fig. 1. The z axis is along the direction of the incoming (target) nucleon, $\hat{p}_N$, while the y axis is along the normal to the production plane, $\hat{y} = \hat{p}_\pi \times \hat{p}_{\pi\pi}$, where $\hat{p}_\pi$ and $\hat{p}_{\pi\pi}$ are vectors along the incoming beam and outgoing dipion directions of motion, respectively. In this coordinate system the target polarization vector, P_T, has polar and azimuthal angles θ' and ϕ'. The normalized target density matrix is given by

$$\rho^T = \tfrac{1}{2}[I + P_T(\sin\theta'\cos\phi'\sigma_x + \sin\theta'\sin\phi'\sigma_y + \cos\theta'\sigma_z)] . \tag{2}$$

The $\pi\pi$ system density matrix can then be written as

$$\rho^{\pi\pi}_{\mu\mu'} = 2\sum_{\alpha,\alpha',\beta} f_{\mu\beta,\alpha}\,\rho^T_{\alpha\alpha'}\,f^*_{\mu'\beta,\alpha'} \Big/ \sum_{\mu,\alpha,\beta} |f_{\mu\beta,\alpha}|^2 . \tag{3}$$

Comparison of eqs. (2) and (3) shows that it is convenient to define four types of density matrix elements. Let

$$\rho^i_{\mu\mu'} = \sum_{\alpha,\alpha',\beta} f_{\mu\beta,\alpha}\,(\sigma_i)_{\alpha\alpha'}\,f^*_{\mu'\beta,\alpha'} \Big/ \sum_{\mu,\alpha,\beta} |f_{\mu\beta,\alpha}|^2 , \tag{4}$$

* The Jacob and Wick [8] "particle 2" phase convention will not be used here.

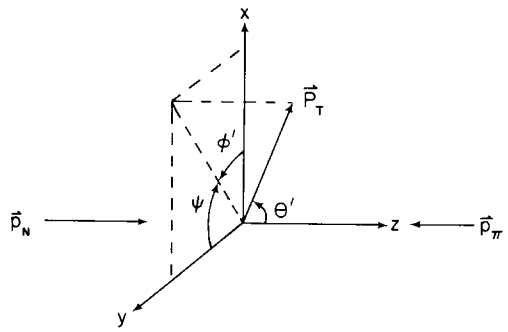

Fig. 1. Definition of the coordinate system used to describe the target polarization vector.

where the superscript i takes on the values o, x, y, or z. Here the σ_i's denote the usual Pauli matrices with $\sigma_0 \equiv I$.

Conservation of parity places the following constraints on the density matrix elements:

$$\rho^i_{-\mu-\mu'} = (-1)^{\mu-\mu'}\rho^i_{\mu\mu'}, \qquad i = o, y,$$

$$\rho^i_{-\mu-\mu'} = -(-1)^{\mu-\mu'}\rho^i_{\mu\mu'}, \qquad i = x, z. \tag{6}$$

Furthermore, hermiticity requires that

$$\rho^i_{\mu\mu'} = \rho^i_{\mu'\mu}{}^* \tag{7}$$

The above equations may be used to derive an expression for the normalized angular distribution of the dipion system. Let (θ, ϕ) denote the polar and azimuthal angles for the decay π^- of reaction (1) in a suitably defined coordinate system *. With these definitions the angular distribution takes the following form **:

$$W(\theta', \phi'; \theta, \phi) = \frac{3}{16\pi^2}\left\{\tfrac{1}{3}\rho_{ss} + \frac{2}{\sqrt{3}}\mathrm{Re}\,\rho_{0s}\cos\theta - \frac{2\sqrt{2}}{\sqrt{3}}\mathrm{Re}\,\rho_{1s}\sin\theta\cos\phi\right.$$

$$+ \rho_{00}\cos^2\theta + \rho_{11}\sin^2\theta - \sqrt{2}\,\mathrm{Re}\,\rho_{10}\sin 2\theta\cos\phi - \rho_{1-1}\sin^2\theta\cos 2\phi$$

$$+ P_T\sin\theta'\cos\phi'\left[\frac{2\sqrt{2}}{\sqrt{3}}\mathrm{Im}\,\rho^x_{1s}\sin\theta\sin\phi + \sqrt{2}\,\mathrm{Im}\,\rho^x_{10}\sin 2\theta\sin\phi\right.$$

$$\left.\left. + \mathrm{Im}\,\rho^x_{1-1}\sin^2\theta\sin 2\phi\right] + P_T\sin\theta'\sin\phi'\left[\tfrac{1}{3}\rho^y_{ss} + \frac{2}{\sqrt{3}}\mathrm{Re}\,\rho^y_{0s}\cos\theta\right.\right.$$

* For s-channel (t-channel) helicity frame density matrix elements θ and ϕ are defined in the $\pi^+\pi^-$ c.m. system with the z axis opposite the outgoing nucleon (along the incoming π^-). In either case the y axis is along the normal to the production plane defined above.

** Here and in the following $\rho_{\mu\mu'} \equiv \rho^0_{\mu\mu'}$.

$$-\frac{2\sqrt{2}}{\sqrt{3}}\,\mathrm{Re}\,\rho^y_{1s}\sin\theta\cos\phi+\rho^y_{00}\cos^2\theta+\rho^y_{11}\sin^2\theta$$

$$-\sqrt{2}\,\mathrm{Re}\,\rho^y_{10}\sin 2\theta\cos\phi-\rho^y_{1-1}\sin^2\theta\cos 2\phi\Big]+P_{\mathrm{T}}\cos\theta'$$

$$\left[\frac{2\sqrt{2}}{\sqrt{3}}\,\mathrm{Im}\,\rho^z_{1s}\sin\theta\sin\phi+\sqrt{2}\,\mathrm{Im}\,\rho^x_{10}\sin 2\theta\sin\phi+\mathrm{Im}\,\rho^z_{1-1}\sin^2\theta\sin 2\phi\right]\Bigg\} \tag{8}$$

There are two relations among the density matrix elements shown above:

$$\rho_{ss}+\rho_{00}+2\rho_{11}=1\,,$$

$$\rho^y_{ss}+\rho^y_{00}+2\rho^y_{11}=P\,, \tag{9}$$

where P is the conventional polarized target asymmetry.

The angular distribution in eq. (8) can also be expanded in terms of spherical harmonics, $Y_{lm}(\theta,\phi)$. Thus, the various density matrix elements in eq. (8) can be expressed in terms of the moments of the angular distribution of the $\pi\pi$ system. These relations are given in the appendix.

For many purposes it is convenient to work with amplitudes which correspond to definite naturality exchange in the t channel. Here $N(U)$ stands for natural (unnatural) parity exchange. Let

$$U^s_{+\pm}=f_{s+,\pm}\quad U^0_{+\pm}=f_{0+,\pm}\,,$$

$$U^1_{+\pm}=(f_{1+,\pm}\mp f_{1-,\mp})/\sqrt{2}\,,$$

$$N^1_{+\pm}=(f_{1+,\pm}\pm f_{1-,\mp})/\sqrt{2}\,. \tag{10}$$

In the event that the $\pi\pi$ moments are measured in the t-channel system (as in ref. [6]), it is necessary to define new amplitudes where the dipion helicity refers to the t channel while the nucleon helicities refer to the s channel. These amplitudes will be denoted by $\tilde{U}^{\mu}_{+\pm}$ and $\tilde{N}^{\mu}_{+\pm}$. They are related to the amplitudes of eq. (10) as follows:

$$\tilde{U}^s_{+\pm}=U^s_{+\pm}\,,\qquad \tilde{N}^1_{+\pm}=N^1_{+\pm}\,,$$

$$\tilde{U}^0_{+\pm}=\cos\chi\,U^0_{+\pm}+\sin\chi\,U^1_{+\pm}\,,$$

$$\tilde{U}^1_{+\pm}=-\sin\chi\,U^0_{+\pm}+\cos\chi\,U^1_{+\pm}\,, \tag{11}$$

where χ denotes the usual vector meson crossing angle.

At present, preliminary results are available [6] for the three $m=0$ moments $2\langle\cos\psi\,Y_{00}\rangle$, $2\langle\cos\psi\,Y_{10}\rangle$, and $2\langle\cos\psi\,Y_{20}\rangle$*. Expressions for the various s-chan-

* Here $\psi=90^\circ-\phi'$ (see fig. 1). These moments have been measured in the t-channel coordinate system for the dipion system.

nel observables are given in the appendix in terms of the amplitudes of eq. (10). Analogous expressions hold for the t-channel observables using the amplitudes of eq. (11).

The twelve observables which may be measured with a transversely polarized target are almost sufficient for a model independent amplitude analysis to be made in terms of transversity amplitudes. The only unknowns are an overall phase and the relative phase between the groups of amplitudes with recoil nucleon transversity up or down.

The magnitudes of the transversity amplitudes obtained from such an analysis have also been presented in [6]. These amplitudes are defined by

$$g_\mu = (\tilde{U}^\mu_{++} + i\,\tilde{U}^\mu_{+-})/\sqrt{2}\,, \qquad h_\mu = (\tilde{U}^\mu_{++} - i\,\tilde{U}^\mu_{+-})/\sqrt{2}, \quad \mu = s, 0\,,$$

$$g_U = (\tilde{U}^1_{++} + i\,\tilde{U}^1_{+-})/\sqrt{2}\,, \qquad h_U = (\tilde{U}^1_{++} - i\,\tilde{U}^1_{+-})/\sqrt{2}\,,$$

$$g_N = (\tilde{N}^1_{++} - i\,\tilde{N}^1_{+-})/\sqrt{2}\,, \qquad h_N = (\tilde{N}^1_{++} + i\,\tilde{N}^1_{+-})/\sqrt{2}\,. \tag{13}$$

Finally, later discussions will be simplified by decomposing the polarization, P, into the components coming from $U^s_{+\pm}$, $U^0_{+\pm}$, $U^1_{+\pm}$, and $N^1_{+\pm}$ which will be denoted by P_s, P_0, P_U, and P_N, respectively. The expressions for these observables are given in the appendix.

3. Model

The model which is used here to study the A_1 exchange terms is an extension of that used to study a variety of reactions, e.g. $\pi^- p \to \rho^0 n$ [5], $\pi^+ p \to (\rho^0, \omega)\Delta^{++}$ [9], and $\pi^- p \to B^0 n$ [10]. In each instance the starting point of the model is to construct conventional Regge pole expressions for the relevant exchanges. In addition to the basic pole terms, it is well known that Regge cuts play an important role. Furthermore, numerous phenomenological analyses have shown that the strength of such terms is correlated with the s-channel net helicity flip, $n = |\mu + \lambda - \lambda'|$, with $n = 0$ cuts strongest. The role of $n \neq 0$ cuts is not well determined, since many successful analyses have been performed in which such terms were absent. In each of the above analyses the $n = 0$ cuts were parametrized in a simple, yet plausible, fashion. The successful description of the data obtained in each case argues against the necessity of including sizeable $n \neq 0$ cuts (see, however, the discussion in sect. 4).

Previous models for reaction (1) have been based on the dominance of π and A_2 exchanges. The new polarization data of ref. [6] show that, in addition to these terms, an exchange which couples to unnatural parity, nucleon helicity non-flip amplitudes is required. This is, presumably, A_1 exchange; previous models must therefore be extended to include this new exchange. A_1 exchange populates U^1_{++}, U^0_{++}, and U^s_{++}. Of these amplitudes, the last two have $n = 0$. Allowance must then be made for Regge cuts in these amplitudes as well. Therefore, the model used here is a straightforward extension of the approach used in refs. [5, 9, 10].

The π-exchange pole terms are parametrized as

$$U^0_{+-} = \sqrt{-t'}\,\beta_\pi \frac{m_\rho}{2}\, e^{C^0_\pi (t-m_\pi^2)}\,\xi_\pi ,$$

$$U^0_{++} = -r_\pi\, U^0_{+-} ,$$

$$U^1_{+-} = -t'\,\beta_\pi\, e^{C^1_\pi (t-m_\pi^2)}\,\xi_\pi , \tag{14}$$

$$U^1_{++} = -r_\pi\, U^1_{+-} ,$$

where $t' = t - t_{\min}$, $r_\pi = \sqrt{t_{\min}/t'}$, and $\xi_\pi = \Gamma(-\alpha_\pi)\,(1 + e^{-i\pi\alpha_\pi})\,(s/s_0)^{\alpha_\pi}$. Here $\alpha_\pi = 0.7(t - m_\pi^2)$ and $s_0 \equiv 1\ \mathrm{GeV}^2$. Notice that the residues at the pion pole are those required for elementary π exchange. However, the separate exponential parameters, C^0_π and C^1_π, effectively allow for the possible presence of a t-channel vector meson helicity one coupling [11]. Note, too, that the π contributions to U^0_{++} and U^1_{++} have been retained.

The A_2-exchange pole terms are parametrized as

$$N^1_{++} = -\sqrt{2}\,\beta_{A_2}\sqrt{-t'}\, e^{C_{A_2} t}\,\xi_{A_2} ,$$

$$N^1_{+-} = \sqrt{-t'}\, R_{A_2}\, N^1_{++} , \tag{15}$$

where

$$\xi_{A_2} = \Gamma(1 - \alpha_{A_2})\,(1 + e^{-i\pi\alpha_{A_2}})\left(\frac{s}{s_0}\right)^{\alpha_{A_2}} ,$$

$\alpha_{A_2} = 0.43 + 0.74\ t$ [12], $\quad R_{A_2} = -4.0\ (\mathrm{GeV}/c)^{-1}$ [13].

There are several theoretical considerations which can be used to motivate the form of the A_1 pole terms. Presumably, there exists an exchange degenerate partner of the A_1 [5,14], called the Z, with $J^{PC} = 2^{--}$. Strong exchange degeneracy, together with the absence of a particle with $J^{PC} = 0^{--}$, requires that the A_1 have a nonsense wrong signature zero (NWSZ) at $\alpha_{A_1} = 0$. A simple parametrization for the A_1 pole terms is

$$U^0_{++} = \beta^0_{A_1}\, e^{C^0_{A_1} t}\,\xi_{A_1} ,$$

$$U^1_{++} = \sqrt{2}\,\beta^1_{A_1}\sqrt{-t'}\, e^{C^1_{A_1} t}\,\xi_{A_1} , \tag{16}$$

where

$$\xi_{A_1} = \Gamma(1 - \alpha_{A_1})\,(1 - e^{-i\pi\alpha_{A_1}})\left(\frac{s}{s_0}\right)^{\alpha_{A_1}}$$

and the A_1 trajectory is chosen to be $\alpha_{A_1} = -0.3 + 0.9\ t$. This particular choice for the A_1 trajectory will be discussed in sect. 4.

One of the Regge cuts appears in $f_{1+,-}$ and, hence, contributes to both N^1_{+-} and U^1_{+-}. It is parametrized as

$$N^1_{+-} = U^1_{+-} = \beta_c \, e^{C_c t} \, s^{\alpha_c} \, e^{-i\pi\alpha_c/2} \, . \tag{17}$$

Previous analyses [5,9] have shown that at small t the cut and the π pole term in U^1_{+-} should be approximately 180° out of phase. Therefore, the cut trajectory has been chosen to be $\alpha_c = 0.0 + 0.4t$. The A_1 cut term in U^0_{++} is likewise parametrized as

$$U^0_{++} = -i \, \beta_c^{A_1} \, e^{C_c^{A_1} t} \, s^{\alpha_c^{A_1}} \, e^{-i\pi\alpha_c^{A_1}/2} \, , \tag{18}$$

where $\alpha_c^{A_1}$ was chosen to be $\alpha_c^{A_1} = -0.4 + 0.45\ t$. This choice was dictated, in part, by considering the energy dependence of $(\rho_{00} + \frac{1}{3}\rho_{ss})d\sigma/dt$ between 6 and 17.2 GeV/c This point will be discussed further below.

Finally, the s-wave amplitudes were obtained using the simple parametrization

$$U^s_{+\pm} = U^0_{+\pm} \, \Gamma e^{i\Delta} , \tag{19}$$

with $\Gamma = 0.4$ and $\Delta = 0.4$ [4]. Note that the same value of Γ is used for both the A_1 and π exchange portions of $U^s_{+\pm}$. This is undoubtedly an oversimplification, but the presently available data are not sensitive to such separate values of Γ.

The above model has been fitted to the previously published data for reaction (1) at 17.2 GeV/c [3], the new polarization data including the transversity amplitude magnitudes [6], and the data for $(\rho_{00} + \frac{1}{3}\rho_{ss})d\sigma/dt$ at 6 GeV/c [7]. The latter data set was included so as to provide an additional constraint on the A_1 cut parameters.

Table 1
The fitted parameter values

β_{A_2}	6.08	$(\mathrm{GeV}/c)^{-1}$
C_{A_2}	0.40	$(\mathrm{GeV}/c)^{-2}$
β_π	51.73	$(\mathrm{GeV}^2/c^3)^{-1}$
C^0_π	2.04	$(\mathrm{GeV}/c)^{-2}$
C^1_π	0.63	$(\mathrm{GeV}/c)^{-2}$
$\beta^0_{A_1}$	411.5	
$C^0_{A_1}$	2.05	$(\mathrm{GeV}/c)^{-2}$
$\beta^1_{A_1}$	67.6	$(\mathrm{GeV}/c)^{-1}$
$C^1_{A_1}$	1.17	$(\mathrm{GeV}/c)^{-2}$
β_c	−67.2	
C_c	1.94	$(\mathrm{GeV}/c)^{-2}$
$\beta_c^{A_1}$	−402.8	
$C_c^{A_1}$	1.53	$(\mathrm{GeV}/c)^{-2}$

The parameter values are given in table 1 and a portion of the resulting fits is shown in figs. 2–4 *.

4. Discussion

The results of the fit to the $m = 0$ polarized target t-channel moments are shown in fig. 2. If A_1 exchange was absent, the equations in the appendix show that these moments would satisfy

$$2\langle \cos\psi \; Y_{10}\rangle = 0 \,,$$

$$2\sqrt{5\pi}\,\langle \cos\psi \; Y_{20}\rangle = -2\sqrt{4\pi}\,\langle \cos\psi \; Y_{00}\rangle \,. \tag{20}$$

Clearly, both of these relations are substantially violated. Furthermore, the A_1 exchange terms used here are capable of describing these observables quite satisfactorily.

The results of the fit are next compared to the transversity amplitude magnitudes of ref. [6] in fig. 3. First, consider $|g_s|$ and $|h_s|$. These quantities are related to P_s as is shown in the appendix. Furthermore, in this model, $P_s = \Gamma^2 P_0$. At small t the π and A_1 contributions to U^s_{+-} and U^s_{++} are about 130° out of phase, thereby giving rise to a large separation between $|g_s|$ and $|h_s|$, corresponding to a large polarization $P_s < 0$. Near $t \approx -0.35\ (\mathrm{GeV}/c)^2$ the two curves cross over, corresponding to a change in sign for P_s. This is due, in this model, to pole-cut interference in the A_1 exchange term. For $-t \gtrsim 0.35\ (\mathrm{GeV}/c)^2$ the cut dominates while at smaller t the pole dominates. The present data do not confirm or contradict this sign change in P_s. However, it is a natural consequence of including an $n = 0$ cut, and it will be difficult to substantially alter this structure.

Next, consider $|g_0|$ and $|h_0|$. The model correctly describes the large separation between these two amplitudes (equivalent to a large negative $\widetilde{P}_0$). This separation indicates that the A_1 has a large t-channel helicity zero coupling. Similarly, the small separation between $|g_U|$ and $|h_U|$ indicates a small t-channel helicity one coupling.

Finally, the large difference between $|g_N|$ and $|h_N|$ is properly described by the model. This separation, corresponding to a large negative P_N, is due to interference between the A_2 pole term in N^1_{++} and the cut in N^1_{+-}.

The results discussed above show that the A_1 exchange terms used here are indeed capable of describing the large unnatural parity exchange contributions to the polarization. The phase of the A_1 exchange pole terms is determined by the trajectory, chosen here to be $\alpha_{A_1} = -0.3 + 0.9t$. This choice corresponds to an A_1 mass of $\sim 1.2\ \mathrm{GeV}/c^2$; not an unreasonable value considering the uncertainty surrounding the properties of the A_1, assuming that it does indeed exist as an identifiable resonance. The magnitude of the polarization, especially in the small t region, is sensitive to the

* The fits to the unpolarized observables not shown here are of excellent quality, yielding a χ^2/DF of 1.1.

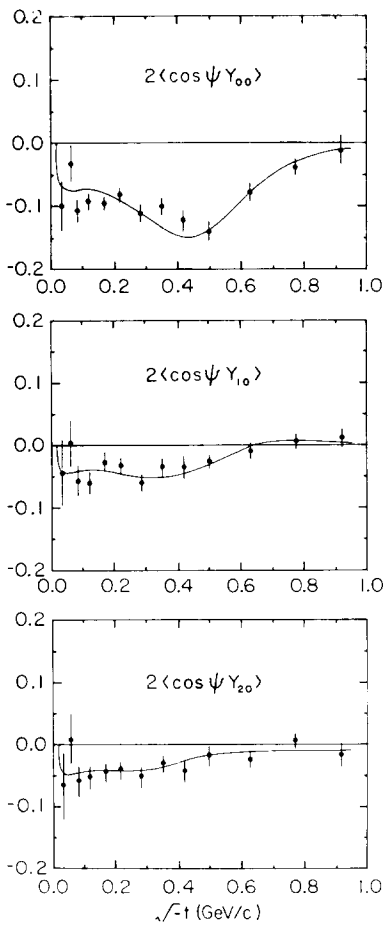

Fig. 2. The results for the $m = 0$, t-channel, polarized target moments.

intercept chosen for the A_1 trajectory. For example, if the A_1 mass was estimated as 1.1 GeV/c^2 and a slope of 0.9 (GeV/c)$^{-2}$ was used for the trajectory, then $\alpha_{A_1} \approx -0.09 + 0.9t$. The NWSZ then occurs at $t \approx 0.1$ (GeV/c)^2 which results in a large suppression of the A_1 exchange terms at small t. This suppression has been used as an argument for the neglect of A_1 exchange in ref. [5]. In ref. [15] an estimate of the polarization expected from A_1 exchange was given which is in reasonable agreement with the data at large t (~20% – 40%). However, the trajectory choice of $\alpha_{A_1} = 0.0 + 0.82\,t$ caused the polarization to be underestimated at small t.

During the actual fitting procedure used here $\alpha_{A_1}(0)$ was varied between –0.5 and –0.05. A broad minimum in the χ^2 was observed for $-0.4 \lesssim \alpha_{A_1}(0) \lesssim -0.2$ so the value of –0.3 used here is merely representative, and some variation is allowed by

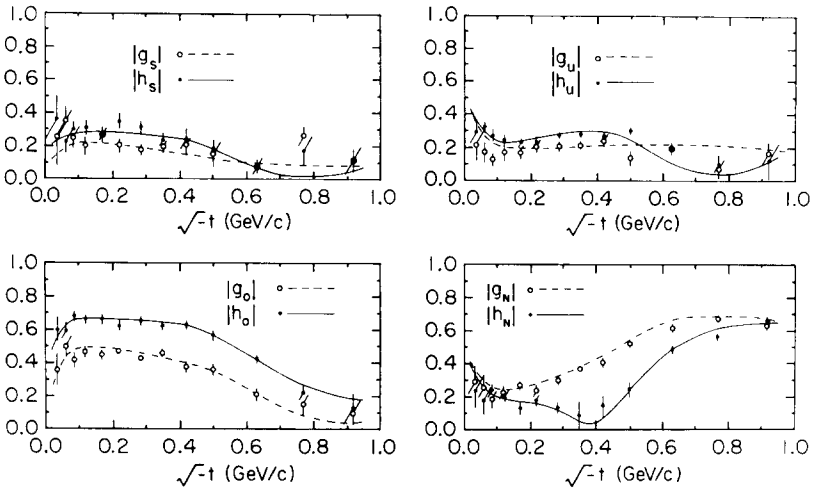

Fig. 3. The results for the transversity amplitude magnitudes. In each t bin, the amplitudes are normalized such that the sum of the squares of the amplitude magnitudes is one.

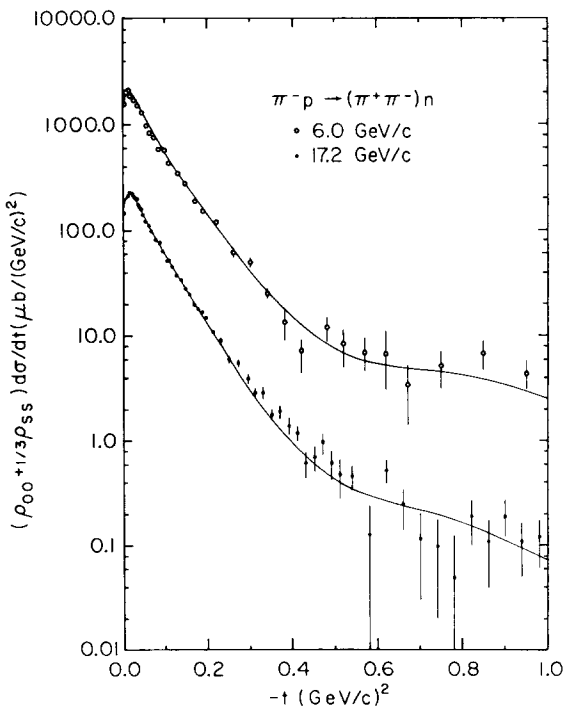

Fig. 4. The results for $(\rho_{00} + \frac{1}{3}\rho_{ss})\ d\sigma/dt$.

the data. Note, however, that if $\alpha_{A_1}(0) << -0.5$, the A_1 phase becomes too close to the π phase, thereby suppressing the polarization. Similarly, the polarization is suppressed by the A_1 NWSZ if $\alpha_{A_1}(0) >> -0.2$.

A characteristic feature of the Regge pole form is that the Regge phase and the energy dependence are correlated. Therefore, further constraints on the A_1 terms could be imposed if some feature of the data at energies other than 17.2 GeV/c could be attributed to them. For sometime it has been known that $\sigma_0 \equiv (\rho_{00} + \frac{1}{3}\rho_{ss})\mathrm{d}\sigma/\mathrm{d}t$ exhibited structure for $-t \gtrsim 0.5$ (GeV/c)^2. At 17.2 GeV/c this is seen as a gentle break while at lower energies the break is sharper. The high statistics data at 6 GeV/c, from an Argonne counter experiment [7], show this structure very clearly. One possible explanation for this break, first suggested in ref. [16], is that the A_1 exchange term in U^0_{++} falls off gradually while the π exchange term in U^0_{+-} is decreasing rapidly. At some point the shape of σ_0 should reflect these two different t dependences. Such is indeed the case in this model, the results of which are shown at 6 GeV/c * and 17.2 GeV/c in fig. 4.

It is clear that the energy dependence of the data is described quite well by the model. This energy dependence, together with the shape of the data, places stringent constraints on the value chosen for the A_1 cut trajectory. The cut must be roughly 180° out phase with the pole at small t in order to obtain the proper pole-cut interference in U^0_{++}. It is this interference which give rise to a dip at $t \approx -0.35$ (GeV/c)^2 followed by a broad secondary maximum (this structure is shown in detail in fig. 5). Furthermore, the A_1 cut trajectory must be sufficiently negative to describe the energy dependence between 6 and 17.2 GeV/c. The resulting trajectory, $\alpha_c^{A_1} = -0.4 + 0.45\,t$, satisfies both of these requirements. The fact that $\alpha_c^{A_1}(0) < \alpha_{A_1}(0)$ may be interpreted as additional log s dependence not contained in the parametrization of eq. (18). It is interesting to note that very similar results, both for the dip location as well as the energy dependence, were obtained using an absorption model prescription for the A_1 cut **.

In fig. 5 the results for $|U^0_{++}|$ and $|U^0_{+-}|$ are compared. The π contribution to $|U^0_{++}|$ is shown by a dashed line. Over the interval $0.1 \lesssim \sqrt{-t} \lesssim 0.6$ GeV/c the A_1 contribution to $|U^0_{++}|$ is about 20% that of the π term in $|U^0_{+-}|$. This feature was noted in ref. [6] and is easily reproduced by the model used here. The A_1 t dependence is comparable to that of the π pole term in this region as a result of the previously mentioned pole-cut interference. $|U^0_{++}|$ has a minimum at $t \approx -0.35$ (GeV/c)^2 followed by a broad maximum at larger t. For $-t \gtrsim 0.5$ (GeV/c)^2 the A_1 term dominates the helicity zero cross section as discussed above.

Also shown in fig. 5 are $|U^1_{++}|$ and $|U^1_{+-}|$. Again, the π contribution to $|U^1_{++}|$ is shown by a dashed line. The sharp minimum in $|U^1_{+-}|$ at $\sqrt{-t} \approx 0.14$ GeV/c is a well known feature of the data and is interpreted as a result of pole-cut interference. $|U^1_{++}|$

* The 6 GeV/c data have been normalized to the 17.2 GeV/c data at the π pole.

** Specifically, an effective absorption profile given by $S_{\mathrm{eff}}(b) = 1 - \mathrm{e}^{-b^2/16}$ was used. This corresponds to complete s-wave ($b = 0$) absorption.

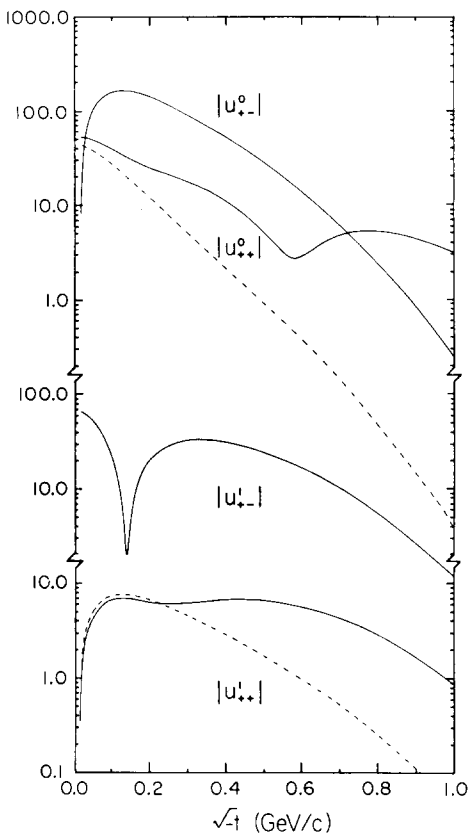

Fig. 5. The results for the unnatural parity, p-wave, amplitude magnitudes. The dashed lines give the π exchange contribution to $|U^0_{++}|$ and $|U^1_{++}|$.

is dominated by π exchange for $\sqrt{-t} \lesssim 0.2$ GeV/c with A_1 exchange dominating in the larger t region. As t approaches -1.0 (GeV/c)^2 the amplitudes U^1_{++} and U^1_{+-} are seen to become comparable in magnitude.

The results of the model discussed above can be compared to those obtained with another model in ref. [6]. The model used there allowed for only a t-channel helicity zero A_1 coupling and the exponential t dependence of the A_1 term was set equal to that of the pion pole. In the present analysis this sharp t dependence emerges naturally as a result of pole-cut interference; no A_1 cut was used in the analysis of ref. [6]. Furthermore, in [6] both the A_2 and A_1 phases were taken as free parameters, assumed to be constant. Here we have used the conventional Regge phases and shown them to be in agreement with the data. Finally, the s dependence of the A_1 exchange term used here has been shown to be compatible with the energy dependence of σ_0 between 6 and 17.2 GeV/c. Thus, the analysis of ref. [6] demonstrated the need for

A_1 exchange while this analysis has shown that a conventional Regge pole and cut prescription gives a good description of the data.

Since A_1 exchange has been demonstrated to be of importance in reaction (1), it will be necessary to examine what effect, if any, its presence will have on previous analyses. Amplitude analyses for reaction (1) [17] have been used to study the structure of the following combinations of amplitudes:

$$|M_0|^2 \equiv |U^0_{++}|^2 + |U^0_{+-}|^2 ,$$

$$|M_-|^2 \equiv |U^1_{++}|^2 + |U^1_{+-}|^2 . \tag{21}$$

If A_1 exchange was absent, then $M_0 \approx U^0_{+-}$ and $M_- \approx U^1_{+-}$, aside from the small π exchange contributions to U^0_{++} and U^1_{++}. In fig. 6 the values for $|M_0|$ and $|M_-|$ obtained in this analysis are shown as solid lines. The dashed lines show the results of setting the A_1 couplings equal to zero. It is readily seen that the effect is negligible for $\sqrt{-t} \lesssim 0.6$ GeV/c. This suggests, then, at least in the ρ region of $\pi\pi$ mass, that the modifications required of previous analyses will be slight in the small t region.

One feature of the A_1 dominated amplitude, U^0_{++}, which has emerged in this analysis is the role played by the A_1 cut. Similar results were obtained using either the parametrization of eq. (18) or a simple absorption model prescription. It is therefore likely that the pole-cut interference obtained here is indeed a feature of the structure of U^0_{++}, although the available data have not yet unambiguously demonstrated this. The structure induced by this interference may be further illustrated by examining the structure of the additional density matrix elements listed in the appendix.

If A_1 exchange is negligible, then several relations between the various observables

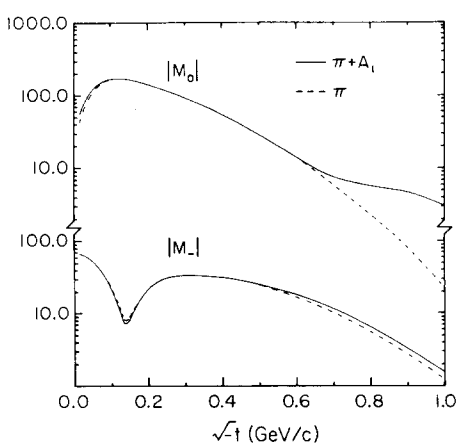

Fig. 6. The model results for $|M_0|$ and $|M_-|$ (solid line). The dashed lines show the results of setting the A_1 couplings equal to zero.

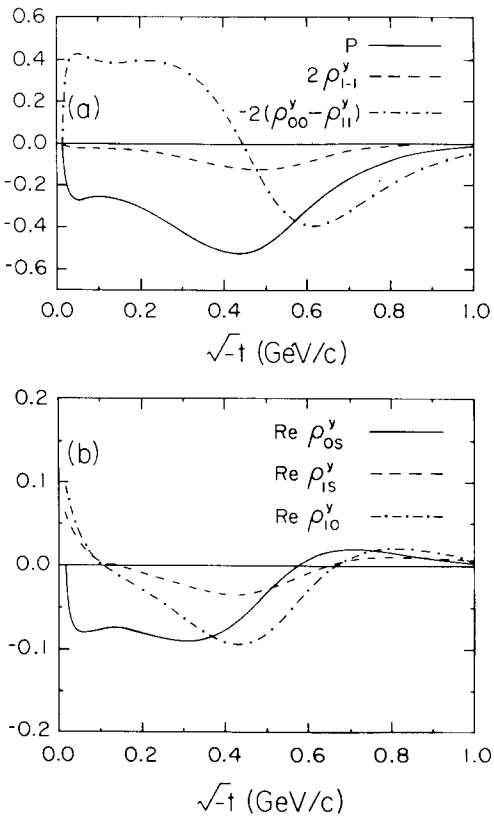

Fig. 7. The results for (a) P, $2\rho^y_{1-1}$, and $-2(\rho^y_{00} - \rho^y_{11})$; (b) Re ρ^y_{0s}, Re ρ^y_{1s}, and Re ρ^y_{10}.

may be obtained *. For example, setting $U^s_{++} = U^0_{++} = U^1_{++} = 0$ results in

$$P = 2\rho^y_{1-1} = -2(\rho^y_{00} - \rho^y_{11}) . \tag{22}$$

In fig. 7a our results for these three quantities are shown as solid, dashed, and dash-dot lines, respectively. All three lines would coincide if eq. (22) was valid. It is clear that the A_1 terms provide a substantial breaking of the relationship in eq. (22). Notice, in particular, that the curves for P and $-2(\rho^y_{00} - \rho^y_{11})$ cross at $\sqrt{-t} \approx 0.6$ GeV/c. This is due to a sign change in P_0 which occurs as a result of the previously discussed A_1 pole-cut interference. Fig. 7b shows the model predictions for Re ρ^y_{0s}, Re ρ^y_{1s}, and Re ρ^y_{10}. In each instance substantial structure is observed. The sign changes occurring near $\sqrt{-t} \approx 0.6$ GeV/c are again due, in part, to the A_1 pole-cut interference in U^0_{++} and U^s_{++}.

* Equivalent relations have been discussed in ref. [18].

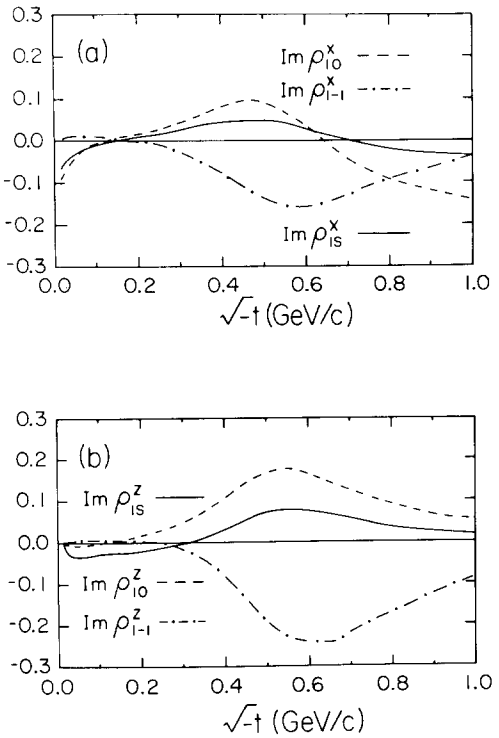

Fig. 8. The model predictions for (a) Im ρ^x_{1s}, Im ρ^x_{10}, and Im ρ^x_{1-1}; (b) Im ρ^z_{1s}, Im ρ^z_{10}, and Im ρ^z_{1-1}.

Finally, fig. 8 shows the predictions for the x and z type density matrix elements. In all cases significant structure exists. However, each observable is given by natural-unnatural parity exchange interference. Thus, the absence of A_1 exchange does not result in any simple relations.

In the above discussion the structure resulting from A_1 pole-cut interference has been stressed. This structure results from the fact that U^s_{++} and U^0_{++} have rapidly changing phases near $\sqrt{-t} \approx 0.6$ GeV/c while the pion dominated amplitudes, U^s_{+-} and U^0_{+-}, have only the smooth phase variation of the $n = 1$ Regge parametrization. This situation could be altered if $n = 1$ Regge cuts play an important role. In particular, the model estimates of ref. [16] suggest that there should be π pole-cut interference resulting in a rapid phase variation, and consequently a dip, near $\sqrt{-t} \approx 0.8$ GeV/c in U^0_{+-} and U^s_{+-}. Such behavior would convert the single zeroes in several observables noted above into either double zeroes or two closely spaced single zeroes. In this analysis the attitude has been taken that the $n = 0$ Regge cuts, together with the various Regge pole terms, will determine the dominant structure of the observables. In this view, the $n = 1$ cuts should play, at most, a minor role and should

not significantly alter the zero structure of the observables. Therefore, if the predictions given above are strongly violated, this may be evidence for the presence of such $n = 1$ cut terms. At the present time this question remains open.

5. Alternatives to A_1 exchange

Thus far, it has been shown that the polarization observed in reaction (1) can be described using a model which incorporates A_1 exchange. However, to date the A_1 has remained an elusive object and some attention must be directed towards alternative mechanisms for populating the amplitudes U^0_{++} and U^1_{++}. The most likely mechamisms would be Regge-pomeron (RP) or Regge-Regge (RR) cuts which are discussed in turn below.

5.1. Regge-pomeron cuts

If RP cuts are generated via a convolution integral, as in the absorption model, then U^0_{++} and U^1_{++} will be zero, provided that the pomeron does not couple to the helicity flip nucleon vertex. An upper limit for such a coupling can be obtained from πN scattering amplitude analyses. The result for the $I = 0$ amplitudes is that the flip/non-flip ratio is of the order of 10–20% [19]. Calculations show that such a value yields an estimate for U^0_{++} which is approximately an order of magnitude too small. Furthermore, consider the phase of a πP cut contributing to U^0_{++}. Since the π amplitude is mostly real and the pomeron term is mostly imaginary, the resulting cut will lie near the real axis in the first or third quadrants depending on the sign of the pomeron flip coupling. However, the phase for U^0_{++} must start out in the fourth quadrant relative to the predominantly real and positive U^0_{+-} in order to describe the polarization correctly. Therefore, RP cuts generated with a flip pomeron will have the wrong magnitude and phase to reproduce the data.

5.2. Regge-Regge cuts

A priori there are a large number of prospective RR terms which can contribute to reaction (1). However, there exist RR selection rules [20,21] which severely constrain such contributions. In particular, these selection rules suggest that RR cuts of the form VV, VT, TV, or TT, where V(T) denotes a vector (tensor) exchange term, are strongly suppressed. The first allowed RR cuts are thus $\pi\rho$ and BA_2. The duality diagrams used in deriving the RR selection rules further constrain these two cuts to appear in the combination $\pi\rho$-BA_2. Of these two terms, the $\pi\rho$ cut is dominant, while the BA_2 is smaller and adds constructively.

In order to obtain an order-of-magnitude estimate for this RR cut combination, the standard convolution prescription has been used. The input π amplitude was taken to be U^0_{+-} while the ρ amplitude was taken to be the ρ flip amplitude from

π^-p elastic scattering. The resulting RR cut contribution to U^0_{++} was more than an order of magnitude smaller than that required to reproduce the observed polarization.

5.3. Z exchange

In refs. [5] and [10] the role of Z exchange in π N $\to \omega$N has been stressed. Presumably the A_1 and Z are exchange degenerate partners, and the A_1 exchange term structure used here reflects this assumption with a NWSZ at $\alpha_{A_1} = 0$. The assumption of exchange degeneracy then predicts that the residues and exponential slopes for A_1 and Z exchange in π^-p $\to \rho^0$n and π^-p $\to \omega$n would be equal. To test this prediction, the model of sect. 3 has been adapted to π^-p $\to \omega$n and fitted to the 6 GeV/c data of ref. [22]. The resulting Z exchange pole parameters are

$$\beta^0_Z = 94.8\,, \qquad \beta^1_Z = 71.9\ (\mathrm{GeV}/c)^{-1}\,,$$

$$C^0_Z = -0.38\ (\mathrm{GeV}/c)^{-2}\,, \qquad C^1_Z = 1.54\ (\mathrm{GeV}/c)^{-2}\,.$$

Comparing these values with the corresponding A_1 parameters in table 1 shows that there is good agreement for the U^1_{++} parameters. For U^0_{++} the Z term appears smaller at $t = 0$ and flatter in t than the corresponding A_1 term. However, the systematic uncertainties attached to β^0_Z and C^0_Z are large since these parameters depend crucially on the assumed form of the cut appearing in U^0_{++}. The lack of polarized target data for ω production prohibits a precise determination of these parameters. Nevertheless, the similarity in the overall contribution of Z exchange in π^-p $\to \omega$n and A_1 exchange in π^-p $\to \rho$n lends support to the concept of approximate $A_1 - Z$ exchange degeneracy.

The values for the B and ρ pole parameters are

$$\beta_B = 53.5\ (\mathrm{GeV}^2/c^3)^{-1}, \qquad C^0_B = 1.52\ (\mathrm{GeV}/c)^{-2}, \qquad C^1_B = -0.47\ (\mathrm{GeV}/c)^{-2}\,,$$

$$\beta_\rho = 9.37\ (\mathrm{GeV}/c)^{-1}\,, \qquad C_\rho = 0.35\ (\mathrm{GeV}/c)^{-2}\,.$$

Comparison with table 1 shows that the ρ term is somewhat larger than the A_2 term. This is the same result found in ref. [5] and also in ref. [9] for π^+p $\to (\rho, \omega)\Delta^{++}$. On the other hand, the π and B parameters are in reasonable agreement, indicating that the amount of π-B exchange degeneracy breaking can be reduced by including A_1 and Z exchanges. This effect has been noted in ref. [9] for π^+p $\to (\rho, \omega)\Delta^{++}$.

6. Conclusions

In this analysis the form of the A_1 exchange amplitudes in reaction (1) has been studied. The model used is a straightforward extension of that used in previous analyses. The model is based on conventional π, A_2, and A_1 Regge pole terms, together with Regge cuts in the $n = 0$ amplitudes. A good description of both the unpolarized and polarized data has been obtained. The major conclusions of this study are as fol-

lows:

(i) Significant A_1 exchange terms are present in the amplitudes of reaction (1). The data are consistent with the use of A_1 pole terms which have the NWSZ structure suggested by duality and exchange degeneracy.

(ii) The results show that both the phase and the energy dependence of the A_1 exchange terms can be described using a reasonable A_1 trajectory.

(iii) The presence of Regge cuts in the $n = 0$ A_1 amplitudes results in significant pole-cut interference which, in turn, gives rise to characteristic zeroes in several of the observables.

(iv) At small t the amplitude magnitudes, $|M_0|$ and $|M_-|$, show only very slight deviations from the values given by neglecting A_1 exchange.

(v) For $-t \gtrsim 0.5$ (GeV/c)^2 A_1 exchange dominates the s-channel helicity zero cross section, σ_0, which, together with the above mentioned pole-cut interference, results in a break in σ_0 at this point. This break becomes less pronounced as the energy increases due to the low trajectories of the A_1 pole and cut.

(vi) The new data may also provide some indication as to the importance of $n = 1$ cuts.

(vii) Estimates of Regge-Regge and Regge-pomeron cuts, using the conventional box diagram, show that these terms are approximately an order of magnitude too small to account for the observed polarization.

(viii) The Z exchange parameters found in an analysis of ω production are in reasonable accord with the corresponding A_1 exchange parameters. Thus, a consistent picture for both ρ and ω production emerges with approximately exchange degenerate π-B, ρ-A_2, and A_1-Z exchanges.

Appendix

In this appendix the observables in eq. (8) are related to the moments of the $\pi\pi$ angular distribution and are then expressed in terms of the amplitudes defined in eq. (10).

$$P = 3\sqrt{4\pi}\langle \sin\theta' \sin\phi' Y_{00}\rangle$$
$$= 4\,\mathrm{Im}[U^s_{++}U^{s*}_{+-} + U^0_{++}U^{0*}_{+-} + U^1_{++}U^{1*}_{+-} + N^1_{++}N^{1*}_{+-}]/\Sigma\,, \tag{A.1}$$

$$\mathrm{Re}\,\rho_{0s} = \sqrt{\pi}\,\langle Y_{10}\rangle = 2\,\mathrm{Re}\,[U^0_{++}U^{s*}_{++} + U^0_{+-}U^{s*}_{+-}]/\Sigma\,, \tag{A.2}$$

$$\mathrm{Re}\,\rho^y_{0s} = 3\sqrt{\pi}\langle \sin\theta' \sin\phi' Y_{10}\rangle = 2\,\mathrm{Im}[U^0_{++}U^{s*}_{+-} - U^0_{+-}U^{s*}_{++}]/\Sigma\,, \tag{A.3}$$

$$\mathrm{Re}\,\rho_{1s} = \sqrt{\pi}\,\langle \mathrm{Re}\,Y_{11}\rangle = \sqrt{2}\,\mathrm{Re}[U^1_{++}U^{s*}_{++} + U^1_{+-}U^{s*}_{+-}]/\Sigma\,, \tag{A.4}$$

$$\mathrm{Im}\,\rho^x_{1s} = -3\sqrt{\pi}\,\langle \sin\theta' \cos\phi' \,\mathrm{Im}\,Y_{11}\rangle = \sqrt{2}\,\mathrm{Im}[N^1_{++}U^{s*}_{+-} + N^1_{+-}U^{s*}_{++}]/\Sigma, \tag{A.5}$$

$$\mathrm{Re}\,\rho^y_{1s} = 3\sqrt{\pi}\,\langle \sin\theta' \sin\phi' \,\mathrm{Re}\,Y_{11}\rangle = \sqrt{2}\,\mathrm{Im}[U^1_{++}U^{s*}_{+-} - U^1_{+-}U^{s*}_{++}]/\Sigma\,, \tag{A.6}$$

$$\mathrm{Im}\,\rho^z_{1s} = -3\sqrt{\pi}\,\langle \cos\theta'\ \mathrm{Im}\ Y_{11}\rangle = \sqrt{2}\,\mathrm{Im}[N^1_{++}U^{s*}_{++} - N^1_{+-}U^{s*}_{+-}]/\Sigma\,, \tag{A.7}$$

$$(\rho_{00} - \rho_{11}) = \sqrt{5\pi}\,\langle Y_{20}\rangle = [2|U^0_{++}|^2 + 2|U^0_{+-}|^2 - |U^1_{++}|^2 - |U^1_{+-}|^2 - |N^1_{++}|^2 - |N^1_{+-}|^2]/\Sigma\,, \tag{A.8}$$

$$(\rho^y_{00} - \rho^y_{11}) = 3\sqrt{5\pi}\,\langle \sin\theta' \sin\phi'\ Y_{20}\rangle = 2\,\mathrm{Im}[2U^0_{++}U^{0*}_{+-} - U^1_{++}U^{1*}_{+-} - N^1_{++}N^{1*}_{+-}]/\Sigma\,, \tag{A.9}$$

$$\mathrm{Re}\,\rho_{10} = \sqrt{\frac{5\pi}{3}}\langle \mathrm{Re}\ Y_{21}\rangle = \sqrt{2}\,\mathrm{Re}[U^1_{++}U^{0*}_{++} + U^1_{+-}U^{0*}_{+-}]/\Sigma\,, \tag{A.10}$$

$$\mathrm{Im}\,\rho^x_{10} = -3\sqrt{\frac{5\pi}{3}}\,\langle \sin\theta' \cos\phi'\ \mathrm{Im}\ Y_{21}\rangle = \sqrt{2}\,\mathrm{Im}[N^1_{++}U^{0*}_{+-} + N^1_{+-}U^{0*}_{++}]/\Sigma\,, \tag{A.11}$$

$$\mathrm{Re}\,\rho^y_{10} = 3\sqrt{\frac{5\pi}{3}}\,\langle \sin\theta' \sin\phi'\ \mathrm{Re}\ Y_{21}\rangle = \sqrt{2}\,\mathrm{Im}[U^1_{++}U^{0*}_{+-} - U^1_{+-}U^{0*}_{++}]/\Sigma\,, \tag{A.12}$$

$$\mathrm{Im}\,\rho^z_{10} = -3\sqrt{\frac{5\pi}{3}}\,\langle \cos\theta'\ \mathrm{Im}\ Y_{21}\rangle = \sqrt{2}\,\mathrm{Im}[N^1_{++}U^{0*}_{++} - N^1_{+-}U^{0*}_{+-}]/\Sigma\,, \tag{A.13}$$

$$\rho_{1-1} = -\sqrt{\frac{10\pi}{3}}\,\langle \mathrm{Re}\ Y_{22}\rangle = [|N^1_{++}|^2 + |N^1_{+-}|^2 - |U^1_{++}|^2 - |U^1_{+-}|^2]/\Sigma\,, \tag{A.14}$$

$$\mathrm{Im}\,\rho^x_{1-1} = 3\sqrt{\frac{10\pi}{3}}\,\langle \sin\theta' \cos\phi'\ \mathrm{Im}\ Y_{22}\rangle = 2\mathrm{Im}[U^1_{++}N^{1*}_{+-} + U^1_{+-}N^{1*}_{++}]/\Sigma\,, \tag{A.15}$$

$$\rho^y_{1-1} = -3\sqrt{\frac{10\pi}{3}}\,\langle \sin\theta' \sin\phi'\ \mathrm{Re}\ Y_{22}\rangle = 2\mathrm{Im}[N^1_{++}N^{1*}_{+-} - U^1_{++}U^{1*}_{+-}]/\Sigma\,, \tag{A.16}$$

$$\mathrm{Im}\,\rho^z_{1-1} = 3\sqrt{\frac{10\pi}{3}}\,\langle \cos\theta'\ \mathrm{Im}\ Y_{22}\rangle = 2\mathrm{Im}[N^1_{+-}U^{1*}_{+-} - N^1_{++}U^{1*}_{++}]/\Sigma\,, \tag{A.17}$$

where

$$\Sigma \equiv \sum_{\mu,\alpha,\beta} |f_{\mu\beta,\alpha}|^2$$

$$= 2[|U^s_{++}|^2 + |U^s_{+-}|^2 + |U^0_{++}|^2 + |U^0_{+-}|^2 + |U^1_{++}|^2 + |U^1_{+-}|^2\,|N^1_{++}|^2 + |N^1_{+-}|^2]$$

$$\frac{\mathrm{d}\sigma}{\mathrm{d}t} = \frac{389\ \mu\mathrm{b}\cdot\mathrm{GeV}^2}{128\,\pi\,m^2 k^2_{\mathrm{lab}}}\ \Sigma\,. \tag{A.18}$$

In the event that a transversely polarized target is used, $\theta' = \frac{1}{2}\pi$. This is the case

for the data of ref. [6]. Furthermore, the target polarization vector is described there by an azimuthal angle, $\psi = \frac{1}{2}\pi - \phi'$. In this instance, the relations in eqs. (A.1)–(A.17) are modified in the following manner:

$$P = 2\sqrt{4\pi}\,\langle \cos\psi\, Y_{00}\rangle\,, \tag{A.19}$$

$$\mathrm{Re}\,\rho^{y}_{0s} = 2\sqrt{\pi}\,\langle \cos\psi\, Y_{10}\rangle\,, \tag{A.20}$$

$$\mathrm{Im}\,\rho^{x}_{1s} = -2\sqrt{\pi}\,\langle \sin\psi\, \mathrm{Im}\, Y_{11}\rangle\,, \tag{A.21}$$

$$\mathrm{Re}\,\rho^{y}_{1s} = 2\sqrt{\pi}\,\langle \cos\psi\, \mathrm{Re}\, Y_{11}\rangle\,, \tag{A.22}$$

$$(\rho^{y}_{00} - \rho^{y}_{11}) = 2\sqrt{5\pi}\,\langle \cos\psi\, Y_{20}\rangle\,, \tag{A.23}$$

$$\mathrm{Im}\,\rho^{x}_{10} = -2\sqrt{\frac{5\pi}{3}}\,\langle \sin\psi\, \mathrm{Im}\, Y_{21}\rangle\,, \tag{A.24}$$

$$\mathrm{Re}\,\rho^{y}_{10} = 2\sqrt{\frac{5\pi}{3}}\,\langle \cos\psi\, \mathrm{Re}\, Y_{21}\rangle\,, \tag{A.25}$$

$$\mathrm{Im}\,\rho^{x}_{1-1} = 2\sqrt{\frac{10\pi}{3}}\,\langle \sin\psi\, \mathrm{Im}\, Y_{22}\rangle\,, \tag{A.26}$$

$$\rho^{y}_{1-1} = 2\sqrt{\frac{10\pi}{3}}\,\langle \cos\psi\, \mathrm{Re}\, Y_{22}\rangle\,. \tag{A.27}$$

It is convenient to separate the polarization, P, into its component parts by defining

$$P = P_s + P_0 + P_U + P_N\,,$$

with

$$P_s = 4\,\mathrm{Im}\, U^{s}_{++}U^{s\,*}_{+-}/\Sigma\,, \tag{A.28}$$

$$P_0 = 4\,\mathrm{Im}\, U^{0}_{++}U^{0\,*}_{+-}/\Sigma\,, \tag{A.29}$$

$$P_U = 4\,\mathrm{Im}\, U^{1}_{++}U^{1\,*}_{+-}/\Sigma\,, \tag{A.30}$$

$$P_N = 4\,\mathrm{Im}\, N^{1}_{++}N^{1\,*}_{+-}/\Sigma\,. \tag{A.31}$$

Similar quantities may be defined using the amplitudes in eq. (11). These quantities then have simple expressions in terms of the transversity amplitudes given in eq. (12),

$$\widetilde{P}_s = P_s = 2[|g_s|^2 - |h_s|^2]/\Sigma\,, \tag{A.32}$$

$$\widetilde{P}_0 = 4\,\mathrm{Im}\,\widetilde{U}^{0}_{++}\widetilde{U}^{0\,*}_{+-}/\Sigma = 2[|g_0|^2 - |h_0|^2]/\Sigma\,, \tag{A.33}$$

$$\widetilde{P}_U = 4 \operatorname{Im} \widetilde{U}^1_{++} \widetilde{U}^{1\,*}_{+-} / \Sigma = 2[|g_U|^2 - |h_U|^2]/\Sigma \,, \tag{A.34}$$

$$\widetilde{P}_N = P_N = 2[|h_N|^2 - |g_N|^2]/\Sigma \,. \tag{A.35}$$

Note, too, that $\widetilde{P}_0 + \widetilde{P}_U = P_0 + P_U$.

References

[1] 1973 Tallahassee Conf. on $\pi\pi$ scattering, AIP Conf. Proc. 13 (1973).
[2] G.C. Fox and C. Quigg, Ann. Rev. Nucl. Sci. 23 (1973) 219.
[3] G. Grayer et al., Nucl. Phys. B75 (1974) 189.
[4] P. Estabrooks and A.D. Martin, Nucl. Phys. B79 (1974) 301; B95 (1975) 322; AIP Conf. Proc. 13 (1973).
[5] A.C. Irving and C. Michael, Nucl. Phys. B82 (1974) 282.
[6] H. Becker et al., Paper submitted to 18th Int. Conf. on high energy physics, Tblisi, July 1976.
[7] D.S. Ayres et al., AIP Conf. Proc. 13 (1973) 37.
[8] M. Jacob and G.C. Wick, Ann. of Phys. 7 (1959) 404.
[9] J.F. Owens et al., Nucl. Phys. B94 (1975) 77; B112 (1976) 514.
[10] A.C. Irving and V. Chaloupka, Nucl. Phys. B89 (1975) 345.
[11] C. Michael, Nucl. Phys. B63 (1973) 431.
[12] M.H. Shaevitz et al., Phys. Rev. Letters 36 (1976) 5.
[13] B. Sadoulet, Nucl. Phys. B53 (1973) 135.
[14] A.C. Irving, Nucl. Phys. B105 (1976) 491.
[15] A.C. Irving, Phys. Letters 59B (1975) 451.
[16] R.D. Field and D.P. Sidhu, Phys. Rev. D10 (1974) 89.
[17] P. Estabrooks and A.D. Martin, Phys. Letters 41B (1972) 350.
[18] J.D. Kimel and E. Reya, Phys. Rev. D8 (1973) 1519.
[19] H. Pilkuhn et al., Nucl. Phys. B65 (1973) 460.
[20] R.P. Worden, Phys. Letters 40B (1972) 260.
[21] G.R. Goldstein, Nucl. Phys. B73 (1974) 109.
[22] M.H. Shaevitz et al., Phys. Rev. Letters 36 (1976) 8.